ACS OMEGA

Open Access

http://pubs.acs.org/journal/acsodf

Article

Application of Flue Gas Foam-Assisted Steam Flooding in Complex and Difficult-to-Produce Heavy Oil Reservoirs

Wei Min* and Linpu Zhang

Cite This: *ACS Omega* 2024, 9, 11574−11588

Read Online

ACCESS | Metrics & More | Article Recommendations

ABSTRACT: In order to study the mechanism of improving recovery efficiency of complex difficult-to-recover heavy oil reservoirs and explain the interaction and migration law of flue gas, foam, and steam, this paper designed the experiment of flue gas influence on heavy oil flow and the experiment of flue gas foam displacement in complex difficult-to-recover heavy oil model. The results show that the flue gas has expansion and an energy enhancement effect. Moreover, the interfacial tension of heavy oil can be reduced, and the higher the CO_2 content in flue gas, the more beneficial it is to reduce the interfacial tension. When there is an interlayer in the reservoir, the gas can form a "puncture" in the interlayer, which provides a channel for the subsequent upward expansion of steam, so that the upper part of the interlayer can be used to expand the steam sweep range. The main mechanism of improving heavy oil recovery with flue gas foam is that the foam regulates fluid mobility and improves the thermal sweep efficiency of steam. In addition, the injected foam can emulsify with heavy oil, reduce the viscosity of heavy oil, and improve the fluidity of heavy oil. Finally, the maximum oil production rate increased from 1.809 to 2.455 g/min, and the recovery rate increased from 44.3 to 68.8%.

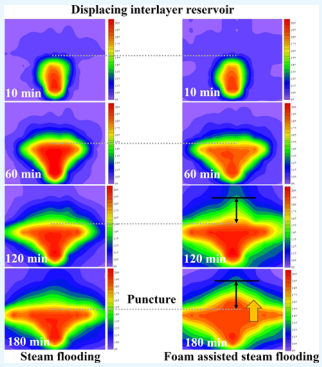

1. INTRODUCTION

Shengli Oilfield plays a decisive role in the stable production of heavy oil reserves in China. The accumulated proven heavy oil reserves of Shengli Oilfield is 4.7×10^8 t, and the deployed reserves of it is 3.64×10^8 t.[1] It should be noted that the heavy oil reservoir of Shengli Oilfield is mainly marginal heavy oil, which is a typical complex and difficult-to-recover heavy oil reservoir. The development difficulties of Shengli Oilfield include the reservoir burial depth of 900−1200 m, the viscosity of oil is more than 10×10^4 mPa·s, the thickness of the oil layer is less than 6 m, the reservoir sensitivity is strong, the water-sensitive permeability retention rate is less than 30%, and the oil−gas ratio is low, only 0.34.[2,3] The above development difficulties make the recovery of heavy oil low. In addition, traditional thermal recovery methods such as steam huff and puff, steam flooding, and SAGD are difficult to effectively develop marginal heavy oil.[4]

Flue gas foam-assisted steam flooding is a new technology proposed in recent years. By injecting multiple components such as steam, noncondensable gas, and chemical agents into the reservoir, the synergistic effect between the multiple components can be used to improve the recovery efficiency of heavy oil and expand the steam sweep range.[5] And it also has a good development effect for marginal heavy oil reservoirs where conventional steam is difficult to effectively utilize. The technology integrates the effects of steam, CO_2, and N_2. The addition of flue gas can not only further reduce the viscosity of crude oil, expand the volume of crude oil, reduce the interfacial tension, and play the role of gas drive but also cooperate with the effect of steam to expand the thermal swept range, reduce steam heat loss, increase formation pressure, and supplement formation energy.[6,7] Since 1960, foam flooding has become the most widely used heavy oil development technology.[8] Different from the conventional single-phase fluid, the gas−liquid two-phase system can effectively improve the injection−production profile and adjust the mobility ratio of the oil displacement system. Foam fluid has various displacement mechanisms such as emulsification and wetting reversal, resulting in easier production of heavy oil.[9] The effects of flue gas foam-assisted steam flooding are affected by many factors such as the viscoelasticity, composition, and type of the fluid.[10] It also makes it possible to develop high-viscosity heavy oil in a complex pore throat structure of formation.

Tong et al.[11] compared the influence of various assisted methods on steam huff and puff by using sandpack model experiments and found that steam injection, accompanied by a certain amount of gas and chemical agent, can effectively improve the steam huff and puff fluidity ratio. Among them, the oil recovery is increased by a flue gas foam of 19%. Zhang et al.[12] conducted a study on the oil recovery evaluation and

Received: November 3, 2023
Revised: January 22, 2024
Accepted: January 26, 2024
Published: February 27, 2024

https://doi.org/10.1021/acsomega.3c08751
ACS Omega 2024, 9, 11574−11588

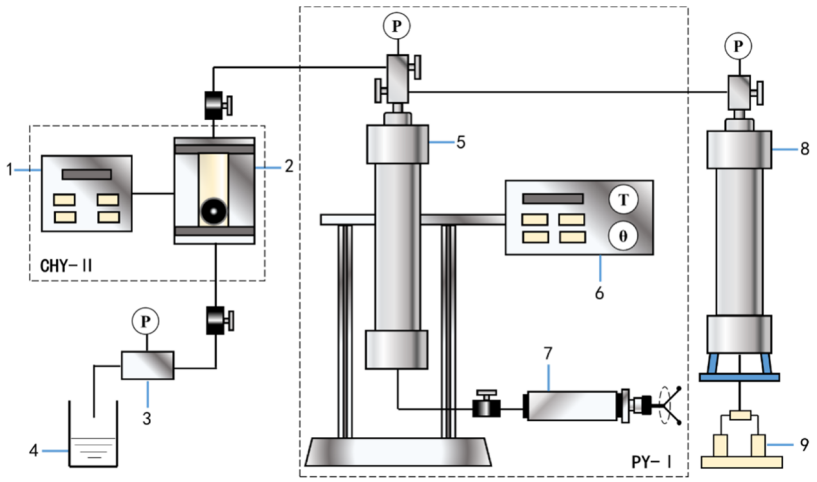

Figure 1. Experimental apparatus for measuring the viscosity of heavy oil influenced by gas (1-CHY-II type falling ball viscometer control panel, 2-viscosity measuring body, 3-back pressure valve, 4-beaker, 5-flue gas and heavy oil mixing vessel, 6-temperature and rotation Angle control panel, 7-hand pump, 8-flue gas container, 9-HPB-30 advection pump).

parameter optimization of combined steam + flue + chemical agent after huff and puff for the oilfield. The results show that flue gas- and chemical-assisted steam flooding have obvious advantages compared with single steam flooding, and the oil recovery is increased by 13.92%. The numerical model results show that when the well spacing is 118 m, the nine-point well pattern is reversed, foam injection volume is 0.2 PV, injection/production ratio is 1:1, and oil recovery can reach 19.25%. Yuan et al.[13] used the high-pressure foam to conduct an experiment on the high-pressure seepage capacity of flue gas foam. The results show that under the formation high-pressure conditions, HY-3 surfactant and flue gas can form a stable foam with strong plugging ability in porous media, and the plugging effect in the heterogeneous core is obviously better than that in the homogeneous core. With the reservoirs' permeability increased, the foam resistance coefficient increased. With the foam injection rate increased, the strength and plugging effect of the foam were increased. With the gas−liquid ratio increased, the foam seepage resistance increased. Basilio and Babadagli[14,15] adopted the idea of injecting flue gas and air and mixing heavy oil to form a foam oil system, which improved the flow property of heavy oil. Meanwhile, the foam in the system increased the displacement pressure and gave the heavy oil a whole viscoelasticity similar to that of foam. Moreover, the presence of heavy oil stabilized the foam structure, improved the flow of the displacement system, and optimized the oil recovery.

There are some research difficulties in flue gas foam-assisted steam flooding, such as the injection components are complex, the multicomponent influences each other, and the seepage characteristics of fluid are not clear. In order to further clarify the interaction between different hot fluids and reveal their migration and distribution laws, the experiments on the influence of flue gas on heavy oil flow and the heavy oil displacement by flue gas foam-assisted steam flooding were designed.

2. EXPERIMENTAL SECTION

2.1. Materials. The viscosity of ground degassed crude oil at 50 °C is 1760 mPa·s, and the density of crude oil is 947.8 kg/m^3. Flue gas N_2 and CO_2 are mixed according to the volume ratio of 4:1, and the purity of nitrogen and carbon dioxide is 99.9%. Distilled water was used in the experiment.

2.2. Experiment on the Influence of Flue Gas on the Flow of Heavy Oil. Flue gas foam-assisted steam flooding technology contains multicomponent gases such as N_2 and CO_2, which have a certain influence[16] on the physical properties of heavy oil. Therefore, the experiment of viscosity of heavy oil affected by multicomponent gases and the experiment of oil−gas interfacial tension were designed, respectively.

2.2.1. Experiment of Multicomponent Gas Affecting Viscosity of Heavy Oil. The experimental equipment, including a PY-I type piston-type high-pressure sampler and a CHY-II-type falling ball viscometer, is shown in Figure 1. Among them, the PY-I piston high-pressure sampler is attached with a rotating system, the highest working temperature is 150 °C, and the control accuracy is ±0.1 °C. The maximum working pressure is 60 MPa, and the accuracy level is 0.4. The maximum working temperature of CHY-II falling ball viscometer is 200 °C, and the control accuracy is ±0.01 °C. The maximum working pressure is 60 MPa, and the measuring range is 0.1−100,000 mPa·s. Hpb-30-type advection pump, the working range is 0−10 mL/min, the accuracy is 0.01 mL/min, and the maximum pressure is 42 MPa. The pressure piston vessel, produced by Jiangsu Haian Petroleum Technology Instrument Co., Ltd., has a volume of 1 L, the maximum pressure is 32 MPa, and the maximum temperature is 150 °C.

The effects of flue gas on viscosity reduction, expansion, and energy increase of heavy oil under different temperature and pressure conditions were measured. The experimental steps are as follows:

(1) Degassed dehydrated crude oil was obtained by electric dehydration of the original oil sample obtained on site.
(2) A certain amount of flue gas was prepared according to Dalton's law of partial pressure, in which the volume fraction of N_2 is 80% and the volume fraction of CO_2 is 20%.
(3) A certain volume of degassed dehydrated crude oil was added to the PY-I piston-type high-pressure sampler.
(4) Under certain temperature conditions, according to the set dissolved gas−oil ratio, a certain volume of flue gas was driven into the sample distributor.

https://doi.org/10.1021/acsomega.3c08751
ACS Omega 2024, 9, 11574−11588

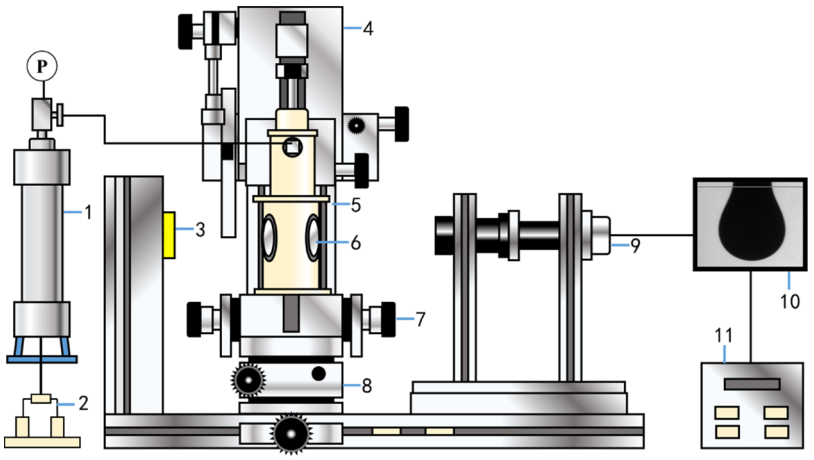

Figure 2. TRACKER tensiomter (1-flue gas container; 2-HLB-30 advection pump; 3-Light source; 4-Motor; 5-interfacial tension test module; 6-visual window; 7-lifting table; 8-translation table; 9-camera; 10-monitor; 11-data storage device).

(5) Determine the saturation pressure under the corresponding conditions: Using the pump back method, through the hand pump the position of the piston in the sample dispenser is changed, so as to change the volume of the oil and gas mixture. The rotation button is pressed, the sample dispenser cylinder rotation up. The mixing speed of oil and gas is accelerated. After the pressure is stable, a series of relationship curves between the pressure and oil mixture volume are drawn to obtain the inflection point of the corresponding pressure for the dissolved gas−oil ratio of the saturated pressure.

(6) The CHY-II type falling ball viscometer was heated up to the experimental temperature. After the temperature was stabilized, a certain volume of crude oil containing dissolved gas was injected into the viscometer by a hand pump to measure its viscosity. The viscosity was measured 5 times, and the average value was taken.

2.2.2. Experiment on the Influence of Multicomponent Gas on Interfacial Tension of Heavy Oil. A TRACKER interfacial rheometer was used to measure the interfacial tension between multicomponent gases and the heavy oil. The experimental device is shown in Figure 2. The TRACKER interface rheometer mainly includes a high-temperature and high-pressure vessel with a window (volume 400 mL, pressure range: 0−20 MPa, temperature range: 0−200 °C), a motor drive system, a 1000 μL microsyringe, a control panel, a gas injection system, a light source, an image acquisition and analysis system, etc.

The experimental steps for measuring the surface tension of flue gas−heavy oil are as follows:

(1) Preparation stage of the experiment: cleaning device and connecting pipeline. The microinjector was filled with test heavy oil and placed in a high-temperature and high-pressure container. The high-temperature and high-pressure container was flushed with 0.3 MPa flue gas 5 times to empty the air inside.

(2) Measurement stage: The high-temperature and high-pressure container was connected with the motor drive system, and the window was adjusted to the appropriate position. The flue gas was injected into the high-temperature and high-pressure container and heated by electric heating. 30−60 min after the pressure and temperature in the container reached a stable value, they were recorded. The oil drop and gas density were input in the test window, the test button was clicked, and a dangling oil drop was formed on the tip of the syringe through the motor drive. At the same time, the shape picture of the oil drop was collected in real time by the camera and transmitted to the computer data acquisition and analysis system to calculate the surface tension between the flue gas and heavy oil.

(3) Change the experimental parameters: under certain temperature and pressure conditions, the surface tension of each flue gas−heavy oil system was measured 3 times, and the average value was taken. Then, the pressure and temperature were changed, step (2) was repeated, the flue gas−heavy oil interfacial tension was measured under different temperatures and pressures, and the experiment was completed.

2.3. Experiment on Improving the Development Effect of Complex and Difficult-to Recover Heavy Oil Reservoirs with Flue Gas Foam-Assisted Steam Flooding. Based on the designed two-dimensional (2D) model, the comparison experiment between steam flooding and flue gas foam-assisted steam flooding was carried out, and the effectiveness of flue gas foam-assisted steam flooding was analyzed from the aspects of temperature field and oil displacement characteristics. In addition, a two-dimensional physical model with an interlayer is also designed to verify the feasibility of flue gas foam-assisted steam flooding in complex and difficult-to-recover heavy oil reservoirs.

2.3.1. Improvement of Super Heavy Oil Reservoirs. The two-dimensional physical model experimental device is shown in Figure 3, including a GL-1 type steam generator, a maximum output steam temperature of 350 °C, and a maximum output pressure of 25 MPa. MKS has a stop valve 2179 A mass flow controller, measuring range is 0−50 sccm, and the accuracy is 1% of the full range. The opening error of the back pressure valve is <0.05 MPa.

The dimensions of the two-dimensional physical model are 40 cm × 50 cm × 1 cm, with a total of 60 temperature measurement points distributed in 6 rows and 10 columns, and the maximum pressure is 3 MPa.

The experimental steps are as follows:

(1) Model preparation stage: A two-dimensional physical model of simulated oil injection with a viscosity of

https://doi.org/10.1021/acsomega.3c08751
ACS Omega 2024, 9, 11574−11588

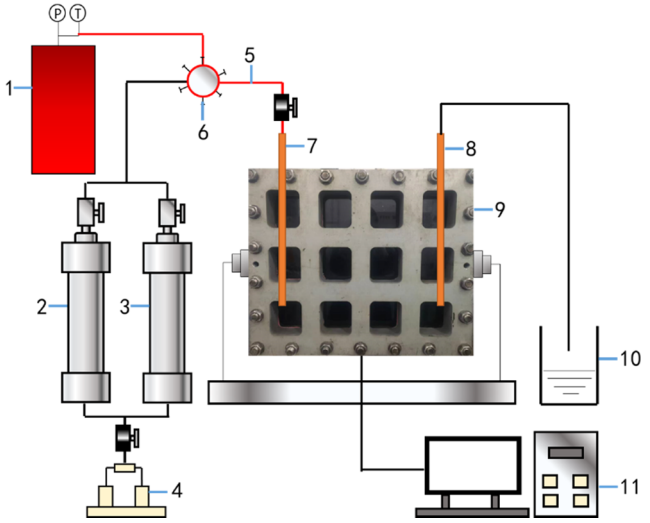

Figure 3. Two-dimensional experimental device (1-GL-1 steam generator; 2-flue gas container; 3- foaming agent container; 4-HLB-30 advection pump; 5- heating belt; 6−6-way valve; 7- production well; 8- injection well; 9- 2D model; 10- beakers; 11- data logger end).

10090 mPa·s at 50 °C was adopted to complete the saturated oil process and simulate the difficult-to-produce heavy oil reservoirs under ultraheavy oil environment. The equipment was connected well, the air tightness of the device was checked, and the measurement of porosity and permeability was completed.

(2) Steam flooding: The injection rate of 10 mL/min (water equivalent) was adopted to inject steam flooding into the model from the injection well, the temperature field changes and the characteristics of liquid production were recorded, and the experiment was stopped when the water content of the produced liquid exceeded 98%.

(3) Flue gas foam-assisted steam flooding: The steam injection speed was set at 10 mL/min (water equivalent), the gas injection speed was set at 10 mL/min, and the foaming agent injection speed was set at 0.5 mL/min. The flue gas foam auxiliary steam flooding experiment was carried out, and the temperature field changes and liquid production characteristics were recorded. When the water content of the produced liquid exceeded 98%, the experiment was stopped.

2.3.2. Break Through the Intermezzanine Reservoir. In the 2D model, clay was used to make strips to act as the intermezzanine reservoir. The interlayer was set 20 cm away from the upper end of the two-dimensional model, as shown in Figure 4.

The experimental procedures were consistent with those described. Steam flooding and flue gas foam-assisted steam flooding were respectively used to conduct displacement experiments in a two-dimensional model with interlayer added, and the temperature field and characteristics of displacement produced liquid were recorded.

3. RESULTS AND DISCUSSION

3.1. Analysis of the Swelling Effect of Multicomponent Gas on Heavy Oil. The dissolved gas−oil ratio of multicomponent gases under different temperatures and pressures was studied by changing the test temperature to 60, 90, and 120 °C and the test pressure to 1−9 MPa, as shown in Figure 5.

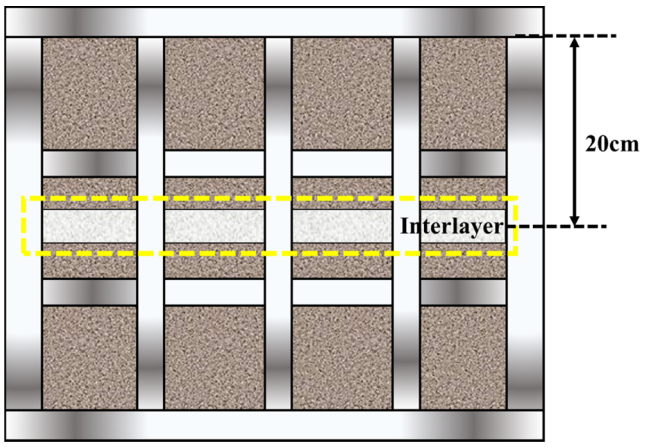

Figure 4. Schematic diagram of the intermezzanine reservoir.

As shown in Figure 5, the research results show that at the same temperature, the dissolved gas−oil ratio of multicomponent gases gradually increases with the increase of pressure, and the increase is nearly linear. However, under the same pressure, the dissolved gas−oil ratio gradually decreases with the increase of temperature because the molecular motion of multicomponent gases is intensified under high-temperature conditions, which is not conducive to its dissolution[17−19] in heavy oil.

The relationship curves of heavy oil volume coefficient with dissolved gas−oil ratio and pressure of multicomponent gases at different temperatures are shown in Figures 6 and 7.

The results show that the volume of the oil−gas mixture expands after the heavy oil dissolves the flue gas. At the same temperature, with the increase of dissolved gas to oil ratio, the volume coefficient first increases linearly and then tends to be gentle. Under the same dissolved gas−oil ratio condition, the volume coefficient of the oil−gas mixture increases gradually with the increase of temperature. In the actual production process, part of the injected flue gas dissolves in the crude oil, which makes the formation oil volume expand, thus increasing the elastic energy[20] of the reservoir.

3.2. Analysis of Viscosity Reduction Effect of Multicomponent Gas on Heavy Oil. The viscosity of crude oil dissolved with multicomponent gases varies with saturation pressure at different temperatures, as shown in Figure 8. On this basis, the viscosity reduction effect of multicomponent gas on heavy oil is analyzed, and the viscosity reduction rate is evaluated, as shown in Figure 9. Viscosity reduction refers to the degree to which the viscosity of heavy oil is reduced after the addition of gas, expressed in the form of percentage. If the initial viscosity of heavy oil is regarded as A and the viscosity of heavy oil after the addition of multicomponent gas is regarded as B, then the viscosity reduction can be defined as $(A-b)/A \times 100\%$.

As shown in Figure 9, viscosity reduction of multiple gases to heavy oil under different temperature and pressure conditions was obtained. The higher the viscosity reduction rate, the lower the viscosity of crude oil, the stronger the flow ability, and the more conducive to the development[21] of heavy oil. The results show that under the same temperature, the saturated pressure increases, the gas dissolution increases, the viscosity reduction rate increases, and the viscosity reduction

https://doi.org/10.1021/acsomega.3c08751
ACS Omega 2024, 9, 11574−11588

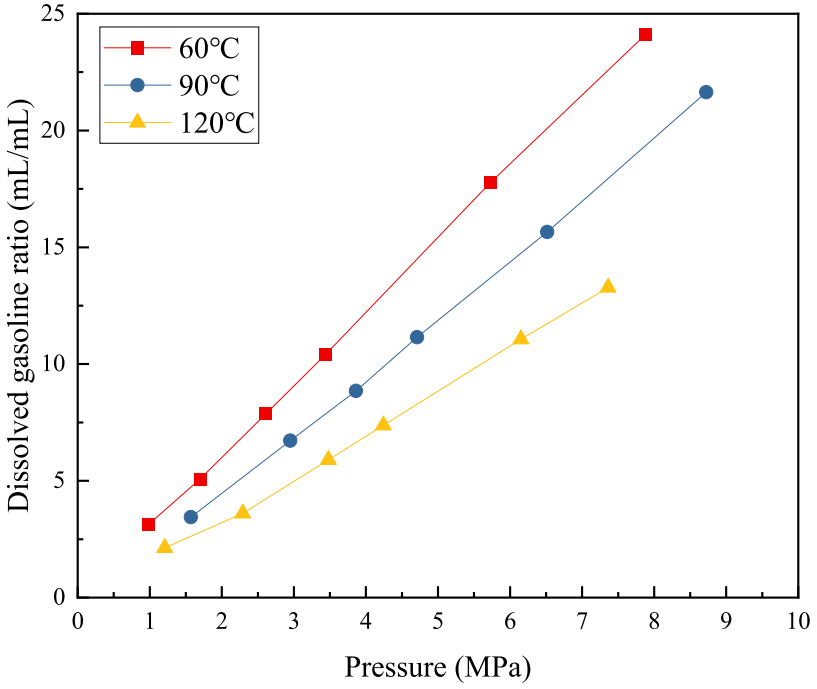

Figure 5. Dissolved gas−oil ratio of multicomponent gases varies with temperature and pressure.

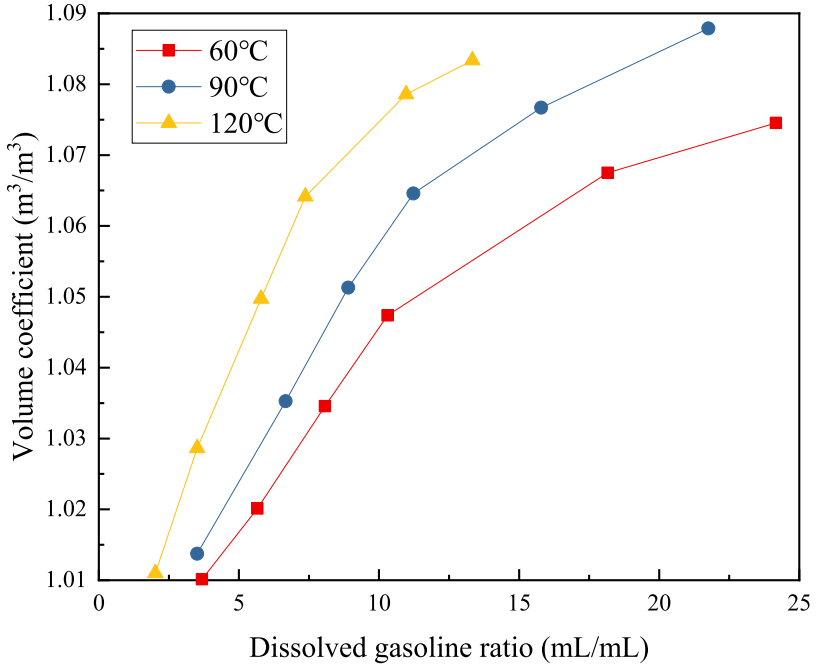

Figure 6. Relationship curves of dissolved gas−oil ratio and volume coefficient at different temperatures.

effect increases. Under the same pressure condition, the higher the temperature, the lower the gas dissolution amount and the lower the viscosity reduction effect. Flue gas has the effect of dissolution and viscosity reduction, but the viscosity reduction effect is weakened at 120 °C compared with 60 °C.

3.3. Interfacial Tension Analysis of Multicomponent Gas and Heavy Oil. Since the flue gas has a certain solubility in the crude oil, after the formation of oil droplets, the flue gas will spread to the crude oil and dissolve until the oil droplets are saturated[22,23] by the flue gas. In order to detect the influence of gas dissolution and diffusion into crude oil on the surface tension, the dynamic surface tension of the flue gas−heavy oil system was measured, and the influence of temperature, pressure, and gas composition on the flue gas−heavy oil interfacial tension was studied, respectively.

Figure 10 shows the dynamic surface tension of multicomponent gas−heavy oil measured at 120 °C and 4 MPa, in which the flue gas composition is 80 mol % N_2 + 20 mol % CO_2, and it is compared with the surface tension of N_2-heavy oil and CO_2-heavy oil. It can be seen that the change in dynamic surface tension can be divided into two stages; the first stage is the fluctuation stage. In the initial stage of gas

https://doi.org/10.1021/acsomega.3c08751
ACS Omega 2024, 9, 11574−11588

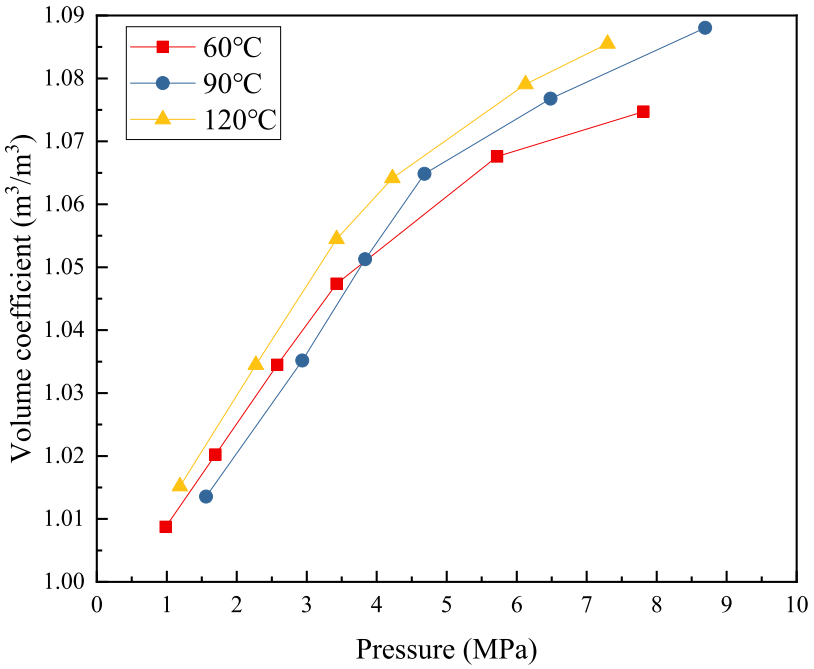

Figure 7. Relationship curves of dissolved gas−oil ratio and volume at different temperatures.

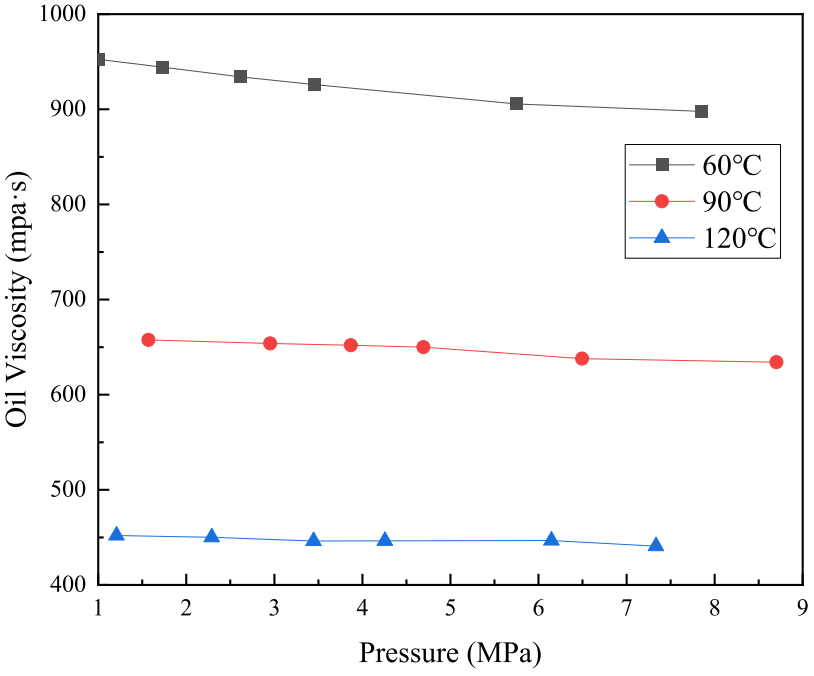

Figure 8. Relation of viscosity of heavy oil with temperature and pressure.

diffusion, the dynamic surface tension fluctuates to a certain extent, about 100 s, indicating that gas diffusion to heavy oil will continue for a period of time. The second stage is the equilibrium stage, and the surface tension of gas−heavy oil fluctuates very little and is almost a constant. Under the same temperature and pressure conditions, the surface tension of N_2-heavy oil is the largest, the surface tension of CO_2-heavy oil is the smallest, and the surface tension of flue gas−heavy oil is between them.

In order to study the effects of temperature and pressure on the equilibrium surface tension of flue gas and heavy oil, experiments were conducted under the conditions of 80, 100, and 120 °C, respectively. Figure 11 shows the curve of the equilibrium surface tension of flue gas and heavy oil with pressure under different temperature conditions.

It can be seen that when the gas pressure increases from 0.2 to 6 MPa at 80 °C, the surface tension of flue gas−heavy oil decreases from 27.31 to 23.53 mN/m, a decrease of 13.84%. At 100 °C, the surface tension of flue gas−heavy oil decreases from 26.10 to 22.26 mN/m, a decrease of 14.71%. At 120 °C, the surface tension of flue gas−heavy oil decreases from 24.75 to 21.75 mN/m, a decrease of 12.12%. Under a certain temperature condition, the equilibrium surface tension of the flue gas−heavy oil system decreases with the increase of

https://doi.org/10.1021/acsomega.3c08751
ACS Omega 2024, 9, 11574−11588

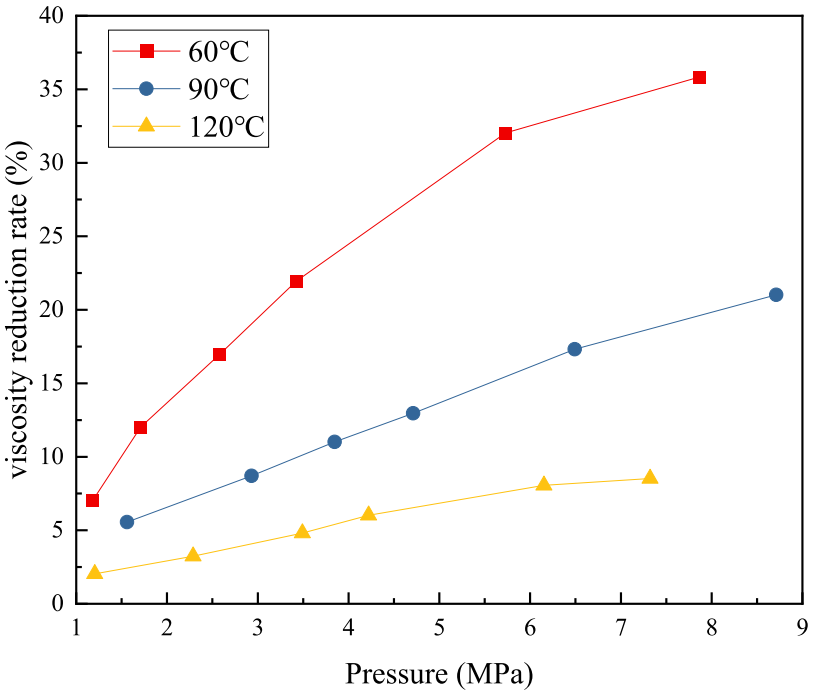

Figure 9. Viscosity reduction with temperature and pressure.

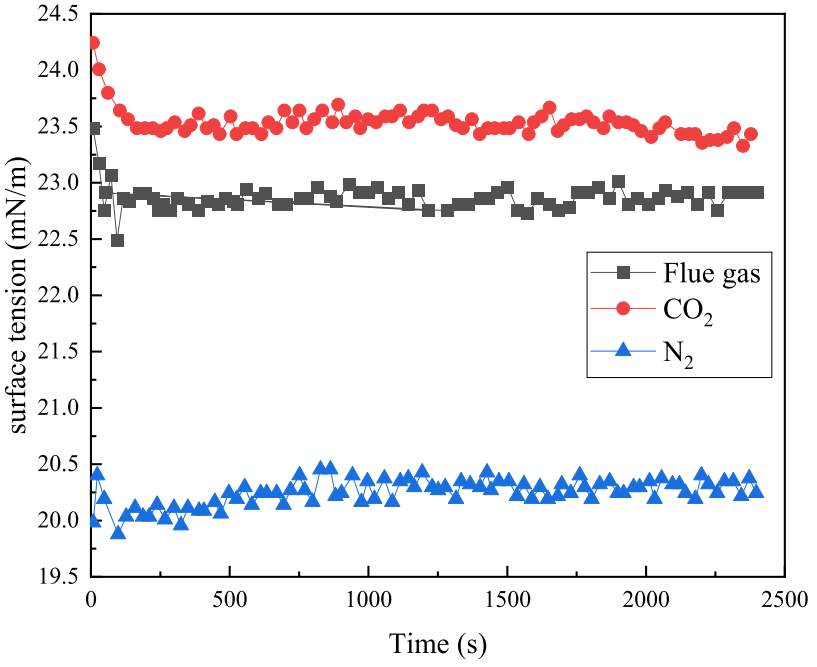

Figure 10. Multicomponent gas–heavy oil interfacial tension (120 °C, 4 MPa).

pressure and shows a good linear relationship. This is because, when the temperature is constant, the pressure increases, the solubility of the flue gas in the heavy oil increases, and the equilibrium surface tension decreases. Under a certain pressure condition, the equilibrium surface tension of the flue gas–heavy oil system decreases with the increase of temperature. This is because the main component of flue gas is N_2, and the solubility of N_2 in heavy oil increases with the increase of temperature.

In the case of a mine, the composition of flue gas is very complex, but the sum of N_2 and CO_2 content in it exceeds 90%.[24−26] During the experiment, the composition of the flue gas is simplified, and the flue gas used is obtained by mixing N_2 and CO_2 in a certain proportion. In the previous study, the composition of the flue gas is 80 mol % N_2 + 20 mol % CO_2. Therefore, the surface tension of flue gas and heavy oil is a comprehensive reflection of the effects of CO_2 and N_2 on the surface tension of heavy oil. Figure 12 shows the curve of CO_2, N_2, flue gas, and heavy oil surface tension changing with pressure at 100 °C.

As shown in Figure 12, at 100 °C, the surface tension between the three gases and heavy oil decreases with an increase in pressure, showing a good linear relationship. At low pressure, the surface tension of the three gases is similar, and

https://doi.org/10.1021/acsomega.3c08751
ACS Omega 2024, 9, 11574−11588

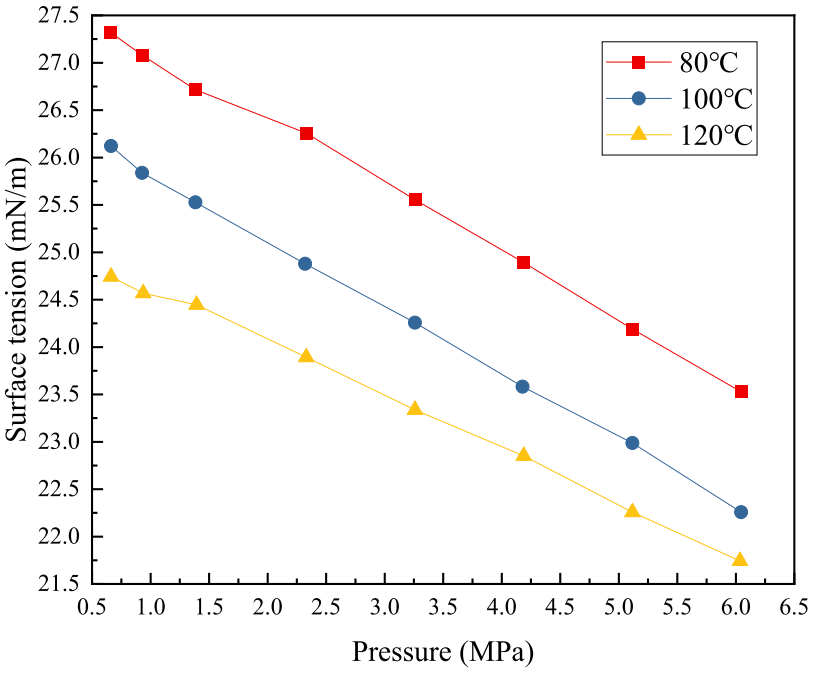

Figure 11. Multicomponent gas−heavy oil interfacial tension changes with temperature and pressure.

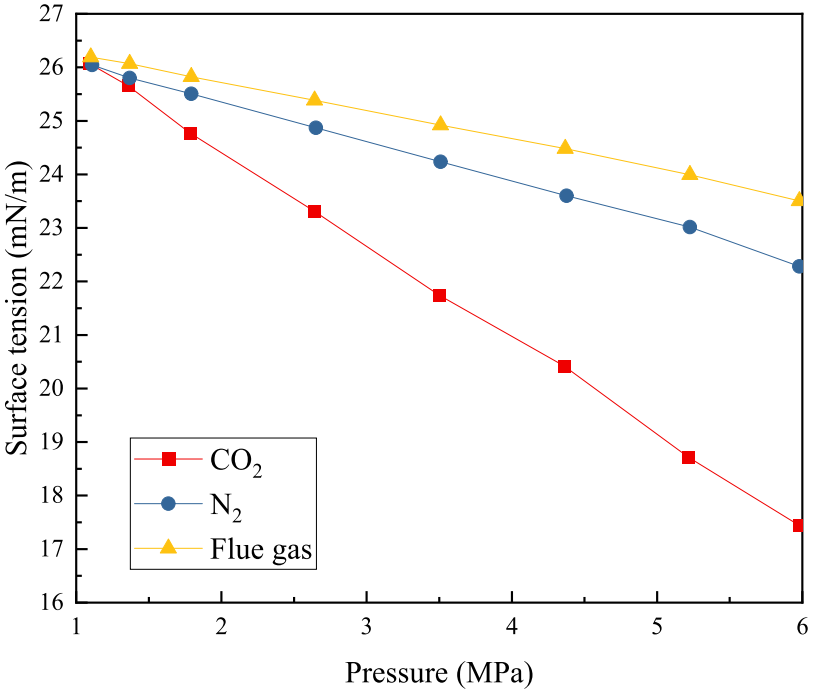

Figure 12. Change of interfacial tension with gas type (100 °C).

the higher the pressure, the greater the surface tension difference of the three gases. When the pressure increases from 1 to 6 MPa, the surface tension of CO_2-heavy oil decreases most significantly, from 26.06 to 17.47 mN/m, a decrease of 32.99%. N_2-heavy oil surface tension decreased from 26.18 to 23.52 mN/m, a decrease of 10.16%. The change of flue gas−heavy oil surface tension was between the two, from 26.10 to 22.26 mN/m, which decreased by 14.71%. This is because the solubility of CO_2 in heavy oil is much greater than that of N_2 under the same temperature and pressure conditions. From the aspect of reducing the surface tension, when other conditions are certain, the higher the CO_2 content in the injected flue gas, the better the oil displacement effect.

3.4. Flue Gas Foam-Assisted Steam Flooding Improves the Temperature Field of Super Heavy Oil Reservoirs. *3.4.1. Improve the Development Effect of Super Heavy Oil Reservoirs.* 30, 60, 120, and 180 min were selected, respectively, and the temperature field distribution and the physical diagram within the four moments were counted, indicating the swept area and the corresponding temperature field distribution in the steam flooding process, as shown in Figure 13.

https://doi.org/10.1021/acsomega.3c08751
ACS Omega 2024, 9, 11574−11588

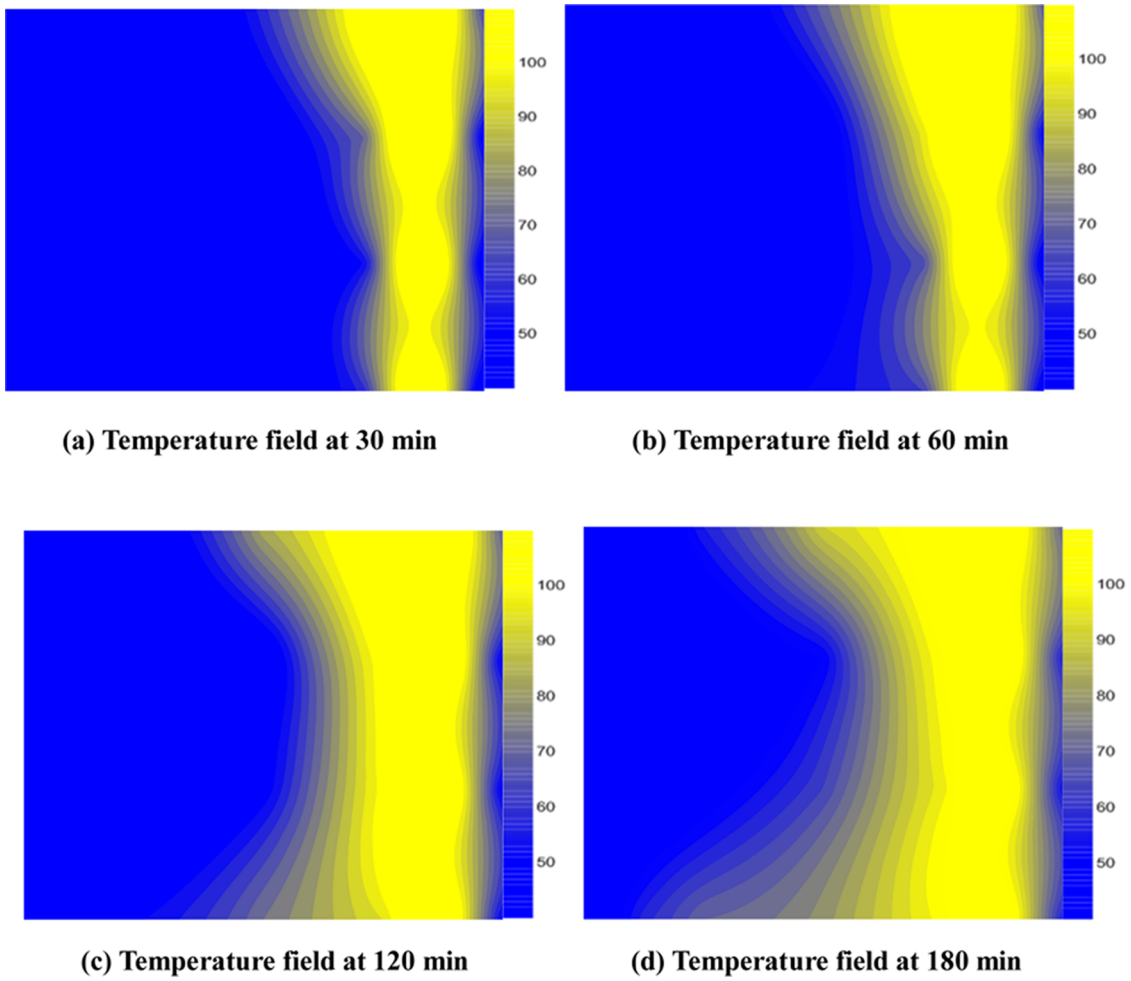

Figure 13. Temperature field of a super heavy oil reservoir by steam flooding.

As shown in Figure 13, in the case of single steam flooding and displacement, steam easily migrated upward due to gravitational overlap, resulting in the steam front moving faster in the upper part of the two-dimensional model than in the lower part.[27] However, the injected steam quickly condenses and percolates downward under the action of gravity in the form of hot water, which mainly migrates along the bottom of the model to the production well.

The temperature field of a super heavy oil reservoir displaced by flue gas foam-assisted steam flooding is shown in Figure 14.

It can be seen that the steam front of flue gas foam-assisted steam flooding has a fast expansion rate in the upper part and a slow expansion rate in the lower part. The spread range and temperature of the lower part of the model increase significantly. Due to the addition of gas, driven by gas, steam also expands up, resulting in the temperature of the upper part of the model of composite hot fluid flooding being obviously higher than the steam flooding. In addition, the gas in the process of seepage, even gas channeling, accelerated the expansion of the steam front. Moreover, the foam inhibits the steam floating up, controls the gas mobility, slows the gas channel, and makes the steam drive front expand more evenly.

According to the comparison diagram of steam thermal swept area and temperature field of super heavy oil reservoirs under two different displacement modes, it can be seen that steam is easy to gather upward under the two displacement modes of steam flooding and flue gas foam-assisted steam flooding due to gravity overlap, resulting in uneven expansion of steam front, fast expansion in the upper part, and slow expansion in the lower part. The addition of gas will produce upward and pointing effects, which aggravate the uneven expansion of steam on the front and the lower part of the model.[28−30] In the process of flue gas foam-assisted steam flooding, the foam can restrain the gas floating up to a certain extent and control the gas mobility, and the steam sweep increases obviously, especially the steam spreading down.

3.4.2. Improving the Development Effect of Reservoirs with Intermezzanine. In the two-dimensional model with interlayer, steam flooding and flue gas foam-assisted steam flooding were carried out, respectively. The temperature field distribution results under different displacement modes are shown in Figures 15 and 16.

As shown in Figures 15 and 16, when steam flooding displaces interlayer reservoirs, the steam chamber cannot develop normally due to the obstruction of the interlayer, so that the upper part of the interlayer cannot be effectively used. However, when gas foam-assisted steam flooding displaces intermezzanine reservoirs, under the action of gravity, gas can float up and form a "puncture" in the intermezzanine, migrate to the area where steam cannot be swept, and finally gather at the top of the reservoir to form a gas cap. The gas "punctures" the intermezzanine, providing a channel for the subsequent

https://doi.org/10.1021/acsomega.3c08751
ACS Omega 2024, 9, 11574−11588

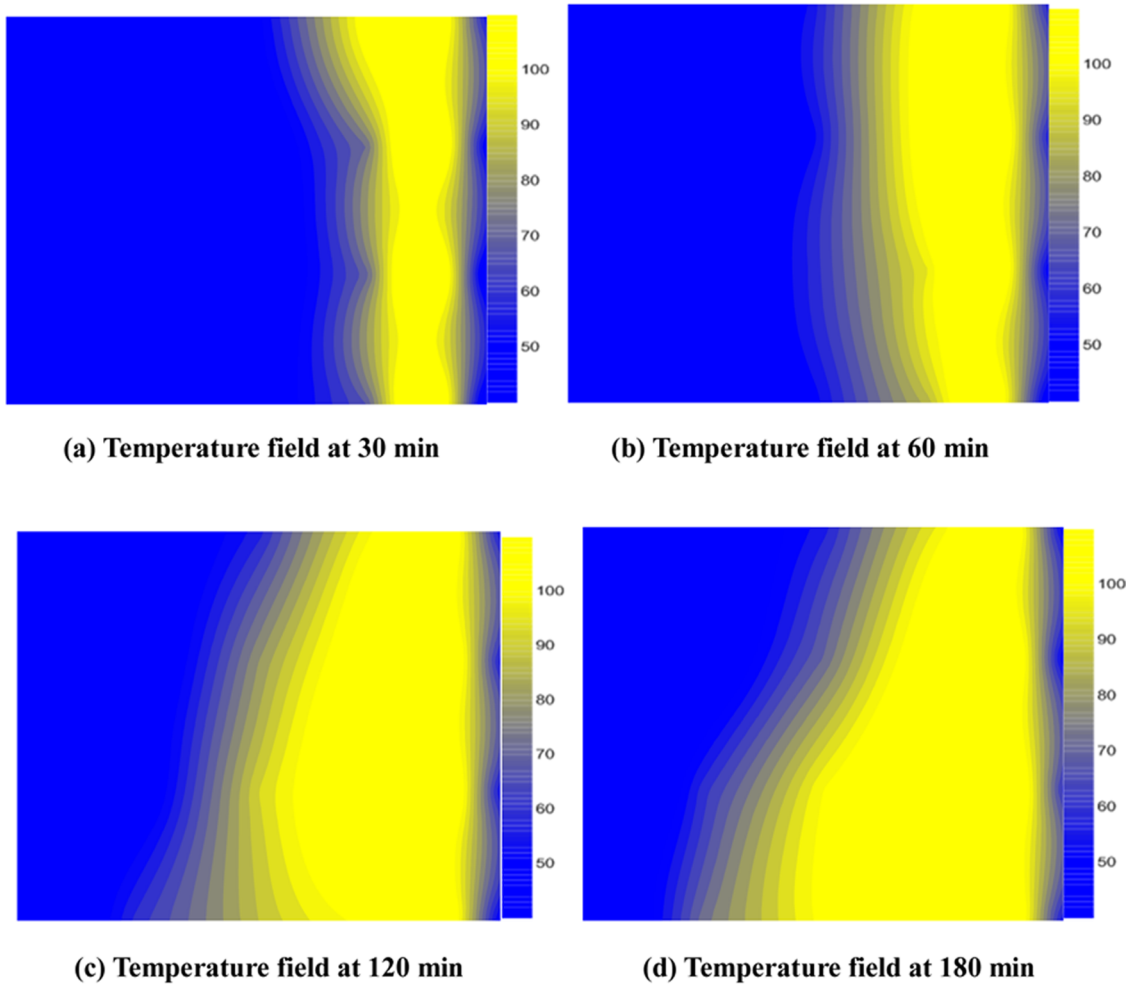

Figure 14. Temperature field of a super heavy oil reservoir driven by flue gas foam-assisted steam flooding.

steam to expand upward, so that the upper part of the intermezzanine can be used to expand the steam sweep range.

3.5. Flue Gas Foam-Assisted Steam Flooding Can Improve the Oil Displacement Law. In the later stage of steam flooding, gas channeling is serious, oil production rate is small, water cut is high, and recovery rate is basically no longer increased.[31−33] Foam has the function of controlling fluidity, which can inhibit gas channeling. At the same time, foam also has the function of reducing the interfacial tension of oil and water and improving the efficiency of oil displacement. Therefore, it is necessary to carry out flue gas foam-assisted steam flooding.

3.5.1. Analysis of Oil Production Rule. Figure 17 compares the oil production rates of steam flooding and flue gas foam-assisted steam flooding.

As can be seen from Figure 17, the oil production rate of steam flooding decays rapidly, and the oil production rate is small in the later stage. In the process of flue gas foam-assisted steam flooding, the oil production rate first decreases and then increases, obviously, indicating that the foam can improve the oil recovery rate to a certain extent. Compared with steam flooding, the maximum oil production rate increased from 1.809 to 2.455 g/min.

Figure 18 shows the form of oil produced in the flue gas foam-assisted steam flooding.

As shown in Figure 18, in the process of flue gas foam-assisted steam flooding, foam and hot water in the injected fluid can form stable emulsification when they come into contact with heavy oil, resulting in severe emulsification of the produced crude oil. It shows that the emulsification of heavy oil is the main mechanism of the flue gas foam to improve the oil displacement efficiency.

3.5.2. Analysis of Gas Production Law. Figure 19 shows the gas production and gas retention in the process of flue gas foam-assisted steam flooding. In order to verify the effect of foam on preventing gas channeling, gas production and gas retention with or without foam injection were compared, respectively, as shown in Figures 20 and21.

As shown in Figures 20 and 21, when foam injection is present, the increased rate of model gas production gradually decreases, and the gas production is gradually lower than that without foam injection, and the gas retention gradually increases. This indicates that foam injection is conducive to controlling gas mobility and reducing gas production rate. In addition, due to the presence of foam, the gas is trapped in the foam, which increases gas retention.[34−37]

The components of gas produced during the initial displacement period, the crossflow period, the foam injection period, and the late displacement period were counted, as shown in Figure 22.

As shown in Figure 22, in the produced gas at the initial stage of displacement, the ratio of nitrogen to nitrogen is 0.86, which is higher than the injection ratio. The proportion of carbon dioxide is relatively low, only 0.14, which is lower than

https://doi.org/10.1021/acsomega.3c08751
ACS Omega 2024, 9, 11574−11588

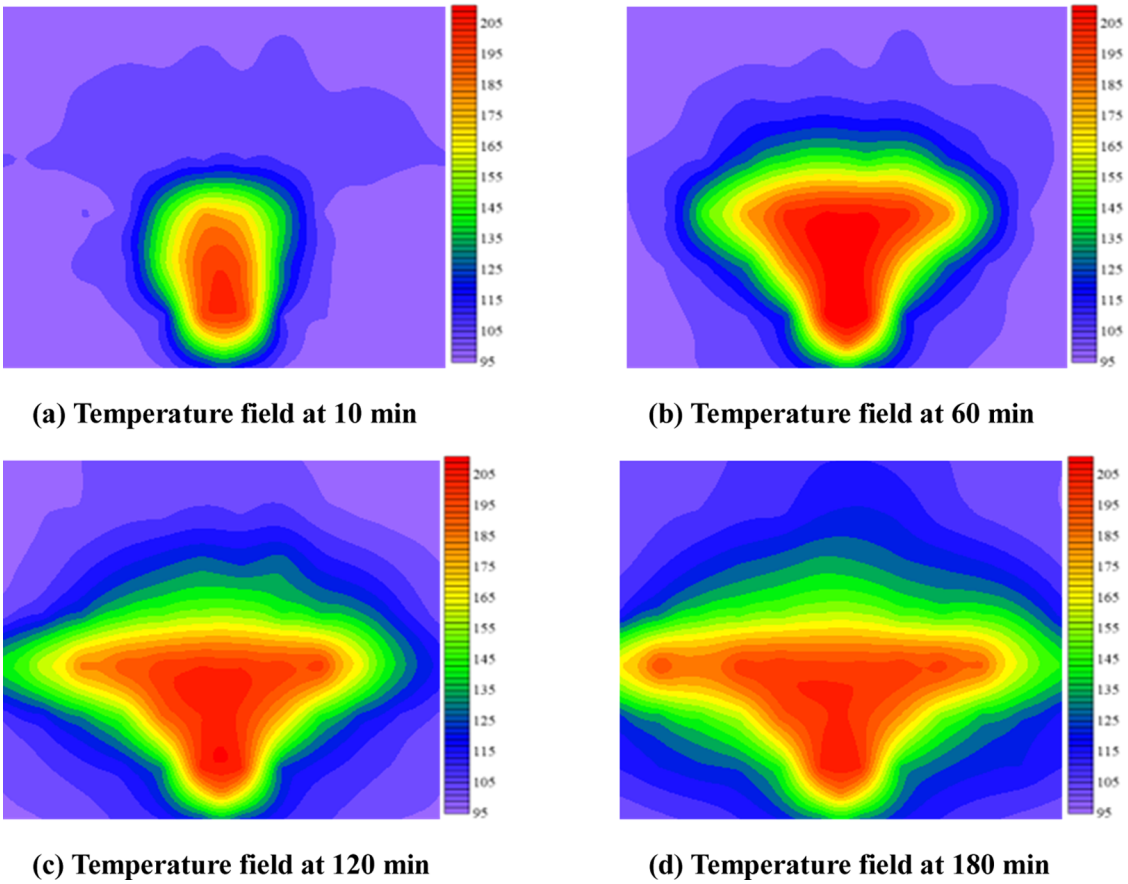

Figure 15. Temperature field of steam flooding displacing interlayer reservoir.

the injection proportion. With the extension of displacement time, the nitrogen ratio in the produced gas gradually decreases and finally decreases to 0.71. The proportion of carbon dioxide in the produced gas gradually increases and finally increases to 0.22.

3.5.3. Analysis of Remaining Oil and Recovery Efficiency. After steam flooding and flue gas foam-assisted steam flooding, oil sands near injection wells and production wells were collected, the oil content of remaining oil in oil sands was calculated statistically, respectively, and the heat distribution in the model during displacement was analyzed, as shown in Figure 23.

As shown in Figure 23, in the case of gas foam-assisted steam flooding, the oil content of the oil sands in the area near the injection well decreased significantly, from 9.76 to 3.79%, and that of the oil sands in the area near the production well decreased from 17.23 to 15.36%, and the overall heavy oil recovery degree in the model was improved. This indicates that more steam heat acts on the front end in the process of gas foam-assisted steam flooding, reducing the crude oil viscosity and improving the oil displacement efficiency there. It shows that the addition of foam can control the fluid fluidity, inhibit the occurrence of channeling flow, and make more steam heat act on the area near the model injection well.

The recovery rates of heavy oil after steam flooding and gas foam-assisted steam flooding are summarized in Figure 24.

The recovery efficiency of steam flooding and flue gas foam-assisted steam flooding was compared, as shown in Figure 24. The recovery efficiency of flue gas foam-assisted steam flooding increased from 44.3 to 68.8%. It is proven that gas foam-assisted steam flooding can effectively improve the recovery rate of heavy oil. The main mechanism of improving heavy oil recovery with flue gas foam is that foam controls fluid mobility, and there is serious channeling in the late stage of pure steam flooding. Although channeling can make a small part of steam percolate to the deep reservoir, the thermal sweep range and efficiency of steam are very low. The flue gas foam-assisted steam flooding controls the fluidity of the hot fluid to a certain extent, which makes the injection well end of the model fully heated and improves the thermal sweep efficiency of the steam. In addition, the injected foam can emulsify with heavy oil, reduce the viscosity of heavy oil, and improve the flow and displacement efficiency of heavy oil.

4. CONCLUSIONS

(1) The dissolution law of multiple gases in heavy oil is that when the temperature is constant, the dissolved gas−oil ratio increases with the increase of pressure. When the pressure is constant, the dissolved gas−oil ratio decreases with the increase of temperature. The multicomponent gas dissolved in the crude oil can make the volume of the crude oil expand and the viscosity decrease, which reflects the expansion and energy increase of the multicomponent gas and the dissolution and viscosity reduction. Under the same temperature and pressure conditions, the surface tension of N_2-heavy oil is the largest, the surface tension of CO_2-heavy oil is the smallest, and the surface tension of flue gas−heavy oil is between the two. From the aspect of reducing the surface tension, the higher the CO_2 content

https://doi.org/10.1021/acsomega.3c08751
ACS Omega 2024, 9, 11574−11588

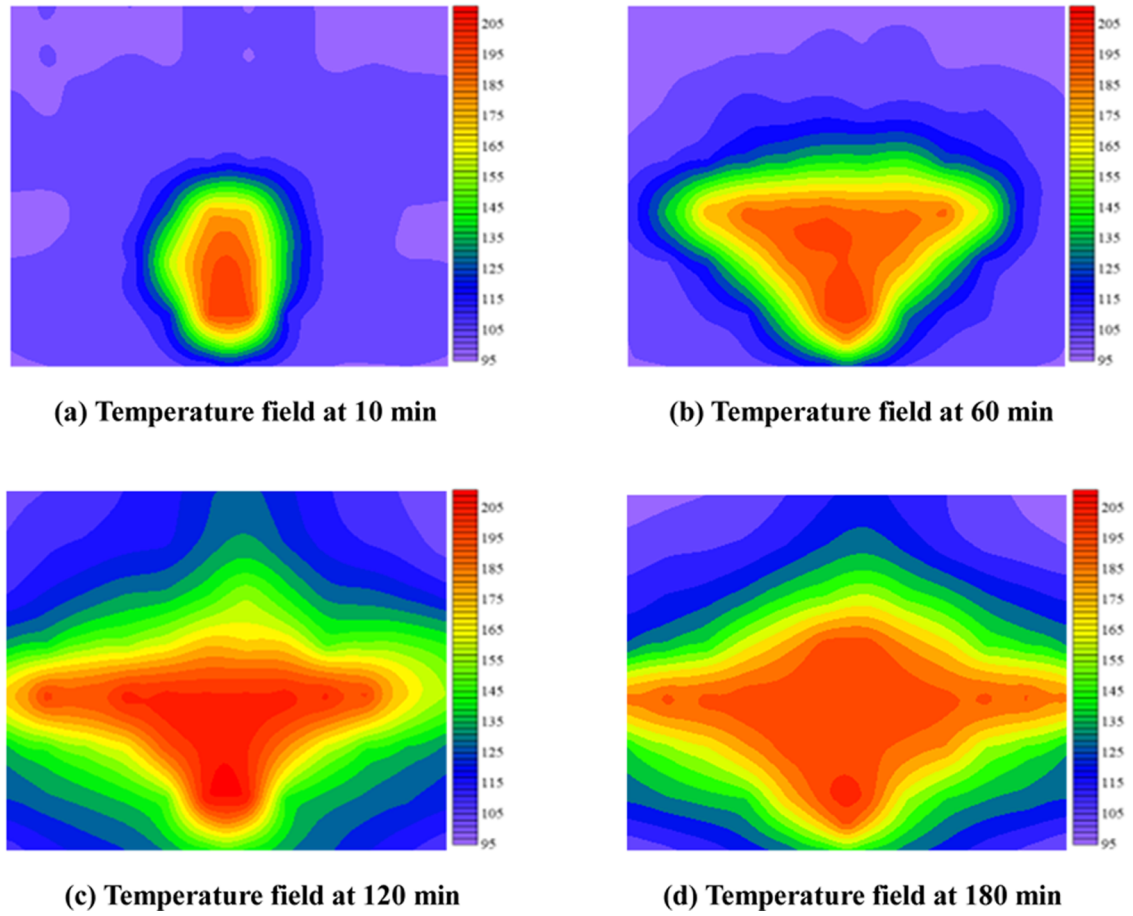

Figure 16. Temperature field of gas foam-assisted steam flooding displacing interlayer reservoir.

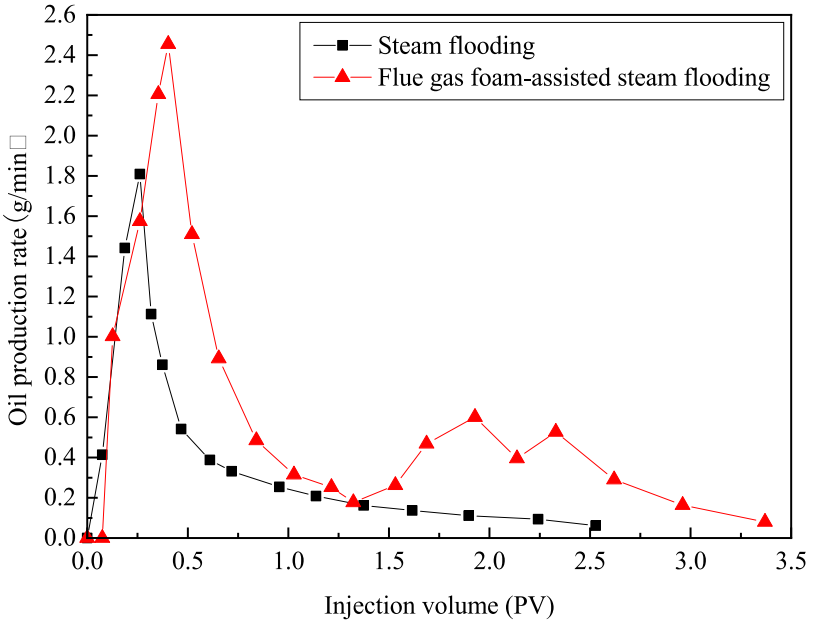

Figure 17. Oil production rates.

in the injected flue gas, the better the oil displacement effect.

(2) According to the two-dimensional model displacement experiment, it can be seen that in the case of single steam flooding, due to the influence of gravity overlap, the steam flooding front expands unevenly, and the steam chamber in the upper part of the model expands faster than that in the upper part of the model. With the flue gas foam-assisted steam flooding, the rising and pointing of the gas expanded the thermal sweep range of

https://doi.org/10.1021/acsomega.3c08751
ACS Omega 2024, 9, 11574−11588

Figure 18. Oil production morphology of flue gas foam-assisted steam flooding.

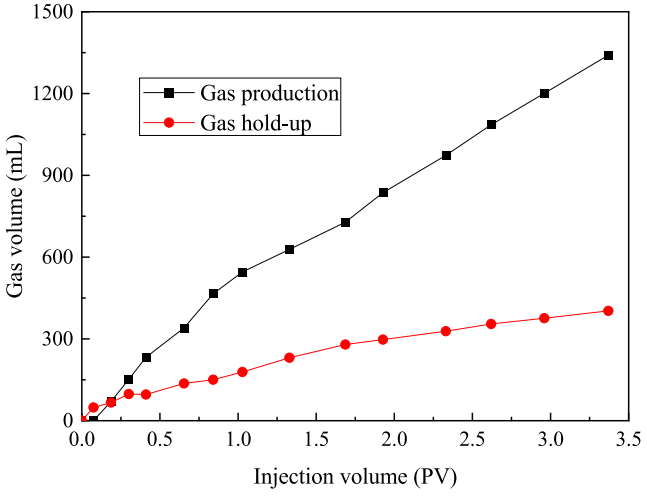

Figure 19. Gas production and gas retention in flue gas foam-assisted steam flooding.

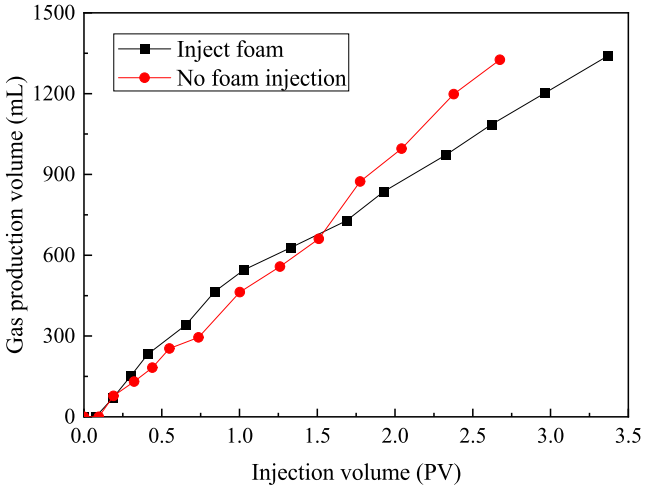

Figure 20. Foam affects gas production.

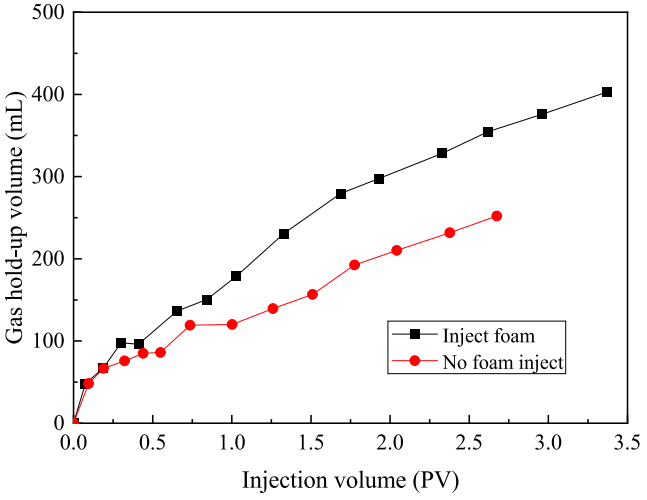

Figure 21. Foam affects gas retention.

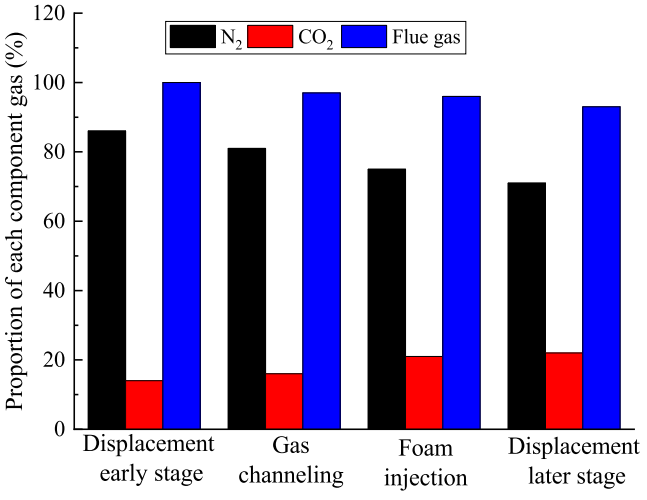

Figure 22. Composition analysis of produced gas in different displacement moments.

the steam. At the same time, the injected foam can control the fluid mobility to the extent of movement, which makes the steam expand to the lower part of the model and improves the steam sweep coefficient. When there are interlayers in the reservoir, the flue gas foam-assisted steam flooding can form a "piercing" in the interlayer, and the gas "piercing" in the interlayer provides a channel for the subsequent upward expansion of steam, so that the upper part of the interlayer can be used to expand the steam sweep range.

(3) The main mechanism of improving heavy oil recovery with flue gas foam is that the foam regulates fluid

https://doi.org/10.1021/acsomega.3c08751
ACS Omega 2024, 9, 11574−11588

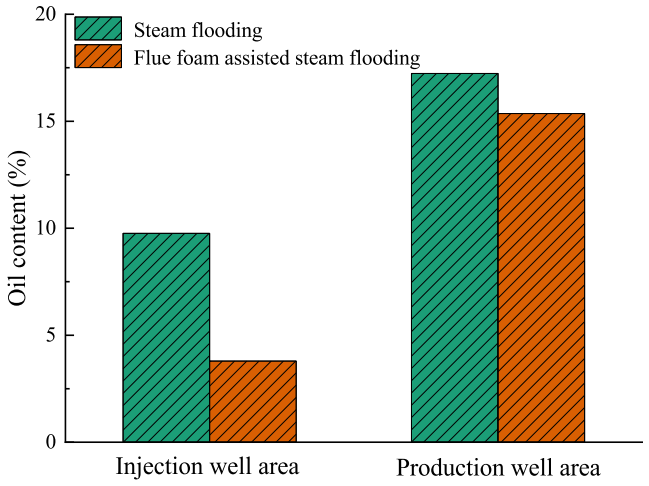

Figure 23. Remaining oil content under different displacement methods.

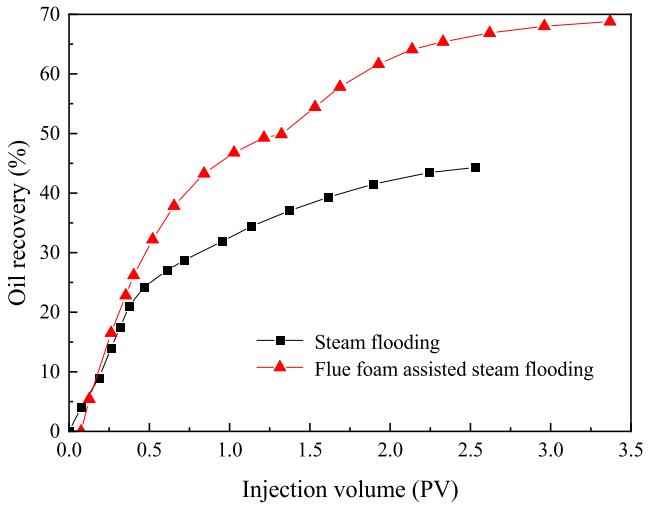

Figure 24. Recovery efficiencies under different displacement methods.

mobility, which makes the injection well end of the model sufficiently heated and improves the thermal swept efficiency of steam. In addition, the injected foam can emulsify with heavy oil, reduce the viscosity of heavy oil, and improve the flow and displacement efficiency of heavy oil. Under the action of flue gas foam-assisted steam flooding, the maximum oil production rate increased from 1.809 to 2.455 g/min, and the recovery rate increased from 44.3 to 68.8%.

AUTHOR INFORMATION

Corresponding Author

Wei Min − *Petroleum Development Center, Shengli Oilfield, Dongying 257001, China;* orcid.org/0009-0003-3317-1981; Email: minwei.slyt@sinopec.com

Author

Linpu Zhang − *Petroleum Development Center, Shengli Oilfield, Dongying 257001, China*

Complete contact information is available at: https://pubs.acs.org/10.1021/acsomega.3c08751

Notes

The authors declare no competing financial interest.

ACKNOWLEDGMENTS

The authors are grateful to the Shandong Engineering Research Center of Carbon Dioxide Utilization and Storage for assistance with their experimental research and for their kind help in this study. The valuable comments made by the anonymous reviewers are also sincerely appreciated.

REFERENCES

(1) Jing, J.; Du, M.; Yin, R.; et al. Numerical study on two-phase flow characteristics of heavy oil-water ring transport boundary layer. *J. Pet. Sci. Eng.* **2020**, *191*, No. 107173.
(2) Cai, N.; Wang, Z.; Zhou, D.; et al. Microgravity exploration method for shallow steam channeling in steam injection heavy oil thermal recovery development areas. *Oil Geophys. Prospect.* **2019**, *54* (1), 235−242.
(3) Shafiei, A.; Dusseault, M. B.; Zendehboudi, S.; et al. A new screening tool for evaluation of steamflooding performance in naturally fractured carbonate reservoirs. *Fuel* **2013**, *108*, 502−514.
(4) Li, H.; Yang, D.; Tontiwachwuthikul, P. Experimental and theoretical determination of equilibrium interfacial tension for the solvent(s)-CO2-heavy oil systems. *Energy Fuels* **2012**, *26* (3), 1776−1786.
(5) Bagci, S.; Kok, M. V. In-situ combustion laboratory studies of Turkish heavy oil reservoirs. *Fuel Process. Technol.* **2001**, *74*, 65−79.
(6) Dong, X.; Shen, L.; Liu, X.; et al. NMR characterization of a tight sand's pore structures and fluid mobility: An experimental investigation for CO2 EOR potential. *Mar. Pet. Geol.* **2020**, *118*, No. 104460.
(7) Li, S.; Wang, Q.; Zhang, K.; et al. Monitoring of CO2 and CO2 oil-based foam flooding processes in fractured low-permeability cores using nuclear magnetic resonance (NMR). *Fuel* **2020**, *263*, No. 116648.
(8) Marquez, A.; Schoeggl, F. F.; Taylor, S. D.; et al. Viscosity of characterized visbroken heavy oils. *Fuel* **2020**, *271*, No. 117606.
(9) Taheri-Shakib, J.; Zojaji, I.; Saadati, N.; et al. Investigating molecular interaction between wax and asphaltene: Accounting for wax appearance temperature and crystallization. *J. Pet. Sci. Eng.* **2020**, *191*, No. 107278.
(10) Islam, M. R.; Hao, Y.; Chen, C. Aggregation thermodynamics of asphaltenes: Prediction of asphaltene precipitation in petroleum fluids with NRTL-SAC-ScienceDirect. *Fluid Phase Equilib.* **2020**, *520*, No. 112655.
(11) Tong, L.; Zhang, G.; Kang, A. Experimental and Numerical Simulation of Improving Steam Throughput by Different Drainage Methods. *Pet. Geol. Recovery Effic.* **2015**, *22* (2), 93−97.
(12) Zhang, X.; Liu, Y.; Che, H.; et al. Study on Improving Heavy Oil Recovery by Steam+Flue Gas+Chemical Agent Composite Flooding. *Sci. Technol. Eng.* **2010**, *10* (10), 175−179.
(13) Yuan, X.; Li, J.; Wang, K.; et al. Experiment on seepage ability of high pressure composite thermal foam in porous media. *Pet. Geol. Oilfield Dev. Daqing* **2009**, *28* (4), 102−104.
(14) Basilio, E.; Babadagli, T. Testing the injection of air with methane as a new approach to reduce the cost of cold heavy oil recovery: An experimental analysis to determine optimal application conditions. *Fuel* **2020**, *265*, No. 116954.
(15) Langevin, D. Influence of interfacial rheology on foam and emulsion properties. *Adv. Colloid Interface* **2000**, *88* (1), 209−222.
(16) Ahemd, S.; Elraies, K. A.; Hashmet, M. R. In *Laboratory study of CO2 foam for enhanced oil recovery: Advanced screening, optimization, and evaluation*, SPE Kingdom of Saudi Arabia Annual Technical Symposium and Exhibition; OnePetro, 2018.
(17) Rafati, R. Application of sustainable foaming agents to control the mobility of carbon dioxide in enhanced oil recovery. *Egypt. J. Pet.* **2012**, *21* (2), 155−163.

(18) Zihan, G.; Zhaomin, L.; Zhengxiao, X.; et al. Microscopic mechanical model analysis and visualization investigation of SiO_2 nanoparticle/HPAM polymer foam liquid film displacing heavy oil. *Langmuir* **2022**, *38* (30), 9166−9185.
(19) Law, D. H.-S.; Yang, Z.-M.; Stone, T. W. Effect of the presence of oil on foam performance: a field simulation study. *SPE Reservoir Eng.* **1992**, *7* (2), 228−236.
(20) Liu, Y.-L.; Zhang, C.; Li, S.-Y.; et al. Study of steam heat transfer enhanced by CO_2 and chemical agents: In heavy oil production. *Pet. Sci.* **2023**, *20* (2), 1030−1043.
(21) Das, D.; Ismail, K. Aggregation and adsorption properties of sodium dodecyl sulfate in water-acetamide mixtures. *J. Colloid Interface Sci.* **2008**, *327* (1), 198−203.
(22) Mehta, S. K.; Bhawna; Kaur, K.; et al. Micellization behavior of cationic surfactant dodecyldimethylethylammonium bromide (DDAB) in the presence of papain. *Colloids Surf., A* **2008**, *317* (1), 32−38.
(23) Inoue, T.; Misono, T. Cloud point phenomena for POE-type nonionic surfactants in imidazolium-based ionic liquids: effect of anion species of ionic liquids on the cloud point. *J Colloid Interface Sci.* **2009**, *337* (1), 247−253.
(24) Páhi, A. B.; Király, Z.; Mastalir, A.; et al. Thermodynamics of micelle formation of the counterion coupled Gemini surfactant Bis(4-(2-dodecyl) benzenesulfonate)-Jeffamine salt and its dynamic adsorption on sandstone. *J. Phys. Chem. B* **2008**, *112* (48), 15320−15326.
(25) D'Andrea, M. G.; Domingues, C. C.; Malheiros, S. V. P.; et al. Thermodynamic and structural characterization of zwitterionic micelles of the membrane protein solubilizing amidosulfobetaine surfactants ASB-14 and ASB-16. *Langmuir* **2011**, *27* (13), 8248−8256.
(26) Taylor, K. C.; Schramm, L. L.; et al. Measurement of short-term low dynamic interfacial tensions: Application to surfactant enhanced alkaline flooding in enhanced oil recovery. *Colloids Surf.* **1990**, *47* (4), 245−253.
(27) Sun, Q.; Li, Z.; Li, S.; et al. Utilization of surfactant-stabilized foam for enhanced oil recovery by adding nanoparticles. *Energy Fuels* **2014**, *28* (4), 2384−2394.
(28) Zihan, G.; Teng, L.; Zhaomin, L.; et al. Experimental investigation on the SiO_2 nanoparticle foam system characteristics and its advantages in the heavy oil reservoir development. *J. Pet. Sci. Eng.* **2022**, *214*, No. 110438.
(29) Chai, M.; Yang, M.; Chen, Z. Systematical study on dimethyl ether as a renewable solvent for warm VAPEX and its significant implications for the heavy oil industry. *Fuel* **2022**, *312*, No. 122911.
(30) Tavakkoli, O.; Kamyab, H.; Shariati, M.; et al. Effect of nanoparticles on the performance of polymer/surfactant flooding for enhanced oil recovery: A review. *Fuel* **2022**, *312*, No. 122867.
(31) Binks, B. P.; Kirkland, M.; Rodrigues, J. A. Origin of stabilisation of aqueous foams in nanoparticle-surfactant mixtures. *Soft Matter* **2008**, *4* (12), 2373−2382.
(32) Dickinson, E.; Ettelaie, R.; Kostakis, T.; et al. Factors controlling the formation and stability of air bubbles stabilized by partially hydrophobic silica nanoparticles. *Langmuir* **2004**, *20* (20), 8517−8525.
(33) Carn, F.; Colin, A.; Pitois, O.; et al. Foam drainage in the presence of nanoparticle-surfactant mixtures. *Langmuir* **2009**, *25* (14), 7847−7856.
(34) Bagci, A. S.; Gumrah, F. In *Effects of CO2 and CH4 addition to steam on recovery of west kozluca heavy oil*, SPE International Thermal Operations and Heavy Oil Symposium and Western Regional Meeting; OnePetro, 2004.
(35) Pang, Z.; Wang, L.; Yin, F.; et al. Steam chamber expanding processes and bottom water invading characteristics during steam flooding in heavy oil reservoirs. *Energy* **2021**, *234*, No. 121214.
(36) Liu, Z.; Ding, Y.; Wang, F.; et al. Thermal insulation material based on SiO_2 aerogel. *Constr. Build. Mater.* **2016**, *122*, 548−555.
(37) Samiur, R. S. M.; Chacko, S. Improved paraffin-deposition -profile estimation in hydrocarbon pipelines and effective mitigation review. *Oil and Gas Facil.* **2013**, *2* (6), 78−85.

https://doi.org/10.1021/acsomega.3c08751
ACS Omega 2024, 9, 11574−11588